Electronic Supplementary Material (ESI) for New Journal of Chemistry.

Electronic Supplementary Information

Lanthanide-based bis-(3,5-dicarboxy-phenyl)terephthalamide metal-organic frameworks: slow relaxation of magnetization and detection of trace Fe^{2+} and Fe^{3+}

Qingfang Lin, Wen Xie, Zhihui Zong, Zicheng Liu, Yuqing Sun, Lili Liang*

Department of Chemistry, Bengbu Medical College, Bengbu 233030, P. R. China.

Contents:

Table S1 Selected bond lengths (Å) and bond angles (°) in **1-2**

			1		
Dy1-O2	2.445(9)	Dy1-O1	2.395(9)	Dy1-O9	2.299(12)
Dy1-O10	2.450(8)	Dy1-O11	2.367(9)	Dy1-O8	2.345(14)
Dy1-O19	2.302(9)	Dy1-O18	2.257(8)	Dy2-O5	2.384(7)
Dy2-O4	2.292(8)	Dy2-O12	2.306(7)	Dy2-O13	2.332(8)
Dy2-O21	2.423(8)	Dy2-O20	2.419(8)	Dy2-O6	2.409(10)
Dy2-O7	2.417(10)				
O2-Dy1-O10	124.7(3)	O1-Dy1-O2	52.9(3)	O1-Dy1-O10	72.1(3)
O9-Dy1-O1	81.6(4)	O9-Dy1-O2	87.9(4)	O9-Dy1-O10	77.9(4)
O9-Dy1-O11	131.3(4)	O9-Dy1-O8	76.1(5)	O9-Dy1-O19	151.7(4)
O11-Dy1-O2	114.7(4)	O11-Dy1-O1	80.0(4)	O11-Dy1-O10	53.6(3)
O8-Dy1-O2	76.8(4)	O8-Dy1-O1	125.4(4)	O8-Dy1-O10	145.3(4)
O8-Dy1-O11	148.3(4)	O19-Dy1-O2	80.3(3)	O19-Dy1-O1	110.2(4)
O19-Dy1-O10	129.8(3)	O19-Dy1-O11	76.9(3)	O19-Dy1-O8	76.3(5)
O18-Dy1-O2	156.0(3)	O18-Dy1-O1	149.6(3)	O18-Dy1-O9	88.9(4)
O18-Dy1-O10	77.6(3)	O18-Dy1-O11	84.9(4)	O18-Dy1-O8	79.3(4)
O18-Dy1-O19	91.7(3)	O5-Dy2-O21	88.5(3)	O5-Dy2-O20	136.3(3)
O5-Dy2-O6	73.3(3)	O5-Dy2-O7	139.4(3)	O4-Dy2-O5	124.5(3)
O4-Dy2-O12	76.5(3)	O4-Dy2-O13	79.7(3)	O4-Dy2-O21	133.9(3)
O4-Dy2-O20	81.8(3)	O4-Dy2-O6	142.2(3)	O4-Dy2-O7	79.8(3)
O12-Dy2-O5	77.5(3)	O12-Dy2-O13	123.5(3)	O12-Dy2-O21	147.8(3)
O12-Dy2-O20	146.1(3)	O12-Dy2-O6	75.9(3)	O12-Dy2-O7	78.0(3)
O13-Dy2-O5	75.4(3)	O13-Dy2-O21	79.1(3)	O13-Dy2-O20	76.6(3)
O13-Dy2-O6	137.7(3)	O13-Dy2-O7	145.1(3)	O20-Dy2-O21	53.6(3)
O6-Dy2-O21	72.4(3)	O6-Dy2-O20	108.5(3)	O6-Dy2-O7	69.6(4)
O6-Dy2-O21	95.5(3)	O6-Dy2-O20	72.7(3)		
			2		
Sm2-O6	2.394(2)	Sm2-O5	2.314(2)	Sm2-O7	2.450(2)
Sm2-O12	2.337(3)	Sm2-O13	2.380(3)	Sm2-O8	2.444(2)
Sm2-O20	2.443(5)	Sm2-O19	2.430(3)	Sm2-O20A	2.400(5)
Sm1-O14	2.486(3)	Sm1 O17	2.305(3)	Sm1 O18	2.302(3)
Sm1-O15	2.394(3)	Sm1-O1	2.467(3)	Sm1-O21	2.364(2)
Sm1-O2	2.424(3)	Sm1-O22	2.327(3)	Sm1-O21A	2.363(3)
Sm1-O2	2.424(3)	Sm1-O22	2.327(3)	Sm1-O21A	2.363(3)
O6-Sm2-O7	88.86(8)	O6-Sm2-O8	136.07(8)	O6-Sm2-O20	72.35(9)
O6-Sm2-O19	140.12(11)	O6-Sm2-O20A	74.10(10)	O5-Sm2-O6	123.72(9)
O5-Sm2-O7	133.81(9)	O5-Sm2-O12	76.91(9)	O5-Sm2-O13	79.37(9)
O5-Sm2-O8	82.14(9)	O5-Sm2-O20	143.62(10)	O5-Sm2-O19	79.99(11)
O5-Sm2-O20A	142.57(12)	O12-Sm2-O6	77.68(9)	O12-Sm2-O7	147.43(9)
O12-Sm2-O13	123.88(9)	O12-Sm2-O8	146.21(8)	O12-Sm2-O20	75.58(8)
O12-Sm2-O19	77.87(10)	O12-Sm2-O20A	75.77(9)	O13-Sm2-O6	74.80(9)
O13-Sm2-O7	79.35(9)	O13-Sm2-O8	76.78(9)	O13-Sm2-O20	136.34(10)
O13-Sm2-O19	144.94(10)	O13-Sm2-O20A	137.65(12)	O8-Sm2-O7	53.21(8)
O20-Sm2-O7	72.09(9)	O20-Sm2-O8	109.06(8)	O19-Sm2-O7	95.22(10)
O19-Sm2-O8	72.56(10)	O19-Sm2-O20	71.33(11)	O20A-Sm2-O7	72.03(10)
O20A-Sm2-O8	107.90(8)	O20A-Sm2-O19	69.64(12)	O17-Sm1-O14	79.00(9)
O17-Sm1-O15	85.54(12)	O17-Sm1-O1	156.09(11)	O17-Sm1-O21	91.21(8)
O17-Sm1-O2	150.49(11)	O17-Sm1-O22	80.29(13)	O17-Sm1-O21A	85.82(9)
O18-Sm1-O14	130.36(10)	O18-Sm1-O17	89.72(10)	O18-Sm1-O15	78.22(11)
O18-Sm1-O1	80.16(10)	O18-Sm1-O21	151.38(9)	O18-Sm1-O2	112.16(12)
O18-Sm1-O22	74.35(14)	O18-Sm1-O21A	148.48(11)	O15-Sm1-O14	52.99(9)
O15-Sm1-O1	113.07(12)	O15-Sm1-O2	80.20(12)	O1-Sm1-O14	123.87(10)
O21-Sm1-O14	77.73(7)	O21-Sm1-O15	130.36(8)	O21-Sm1-O1	87.69(8)
O21-Sm1-O2	78.94(10)	O2-Sm1-O14	71.76(10)	O2-Sm1-O1	52.22(11)
O22-Sm1-O14	147.25(12)	O22-Sm1-O15	149.04(13)	O22-Sm1-O1	76.14(14)
O22-Sm1-O21	77.63(11)	O22-Sm1-O2	123.51(13)	O22-Sm1-O21A	74.14(13)

O21A-Sm1-O14	79.29(9)	O21A-Sm1-O15	132.28(10)	O21A-Sm1-O1	91.56(9)
O21A-Sm1-O2	84.93(11)				

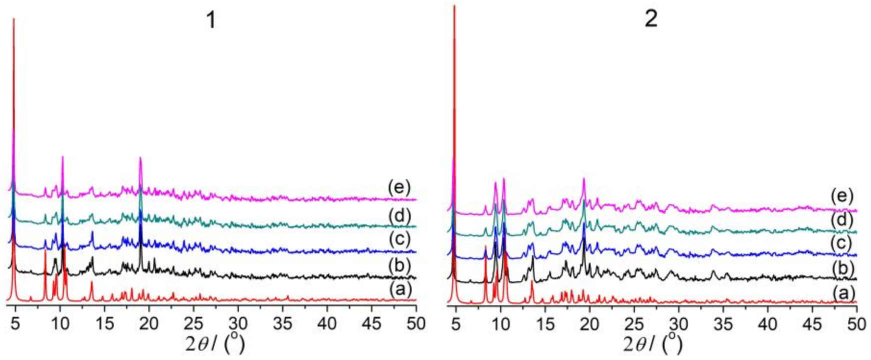

Fig. S1 Powder XRD patterns for **1** and **2**: (a) simulated, (b) synthesized, (c) after soaked in DMF, (d) after soaked in water, (e) after soaked in aqueous solution of Fe^{2+} and Fe^{3+}.

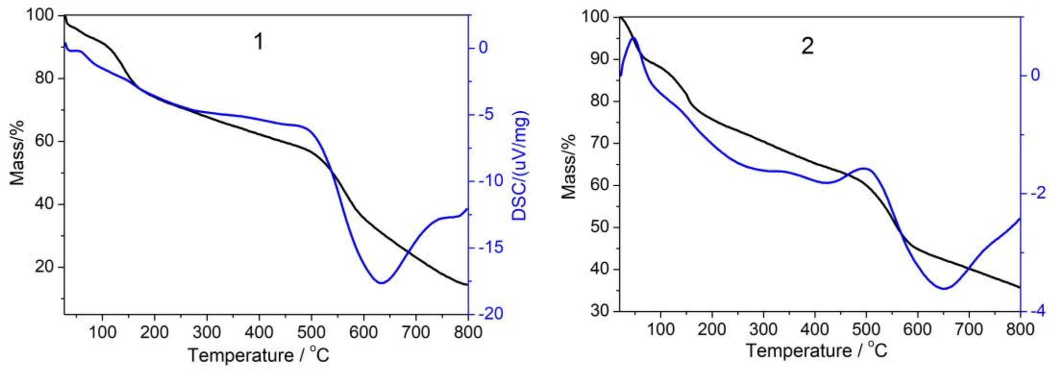

Fig. S2 TGA-DSC curves of **1** and **2** under nitrogen

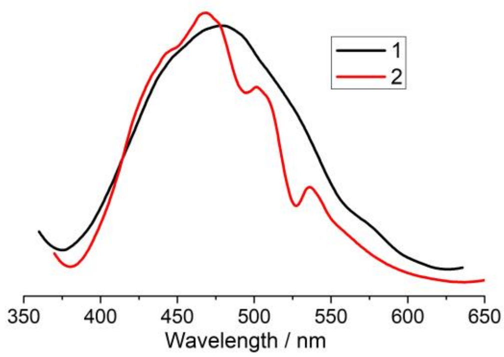

Fig. S3 Solid state fluorescence spectrum of **1** and **2**

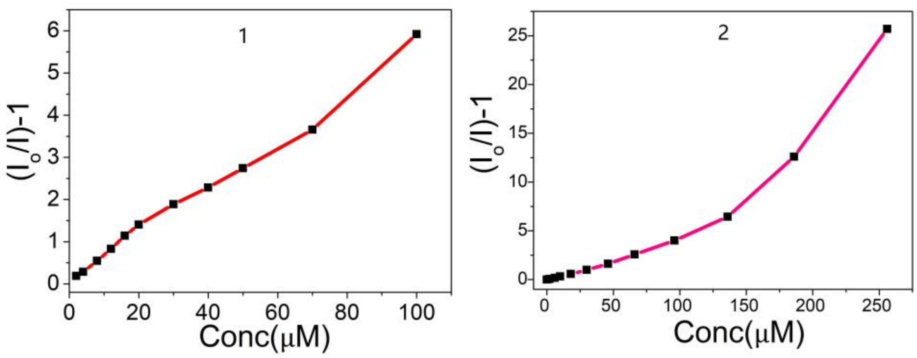

Fig. S4 (a) SV plot of (a) **1** and (b) **2** by gradual addition of Fe^{2+} (0 – 250 μM) in DMF

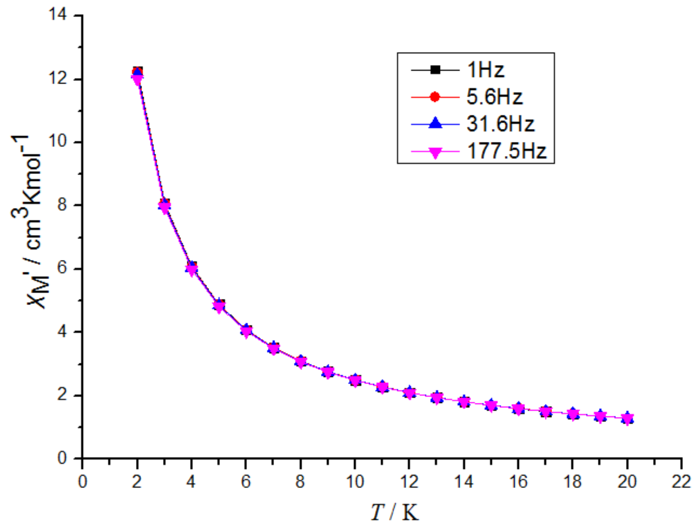

Fig. S5 Temperature dependence of the in-phase (χ_M') ac susceptibility components measured at different frequencies for compound **1** at zero dc field and an oscillation of 2.5 Oe.

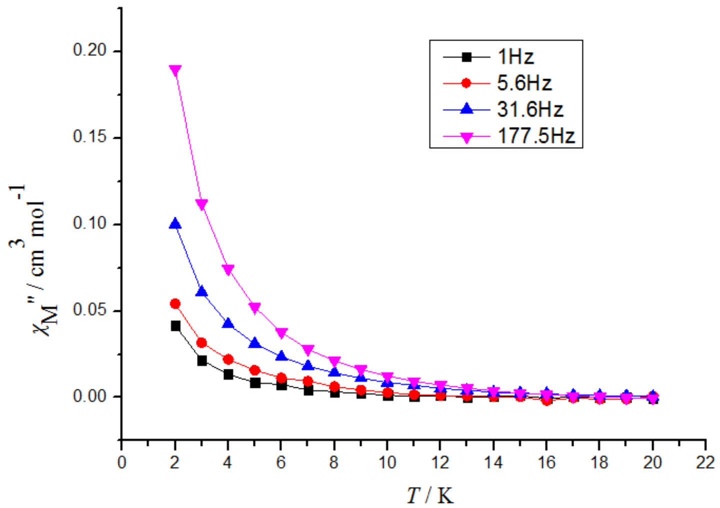

Fig. S6 Temperature dependence of the out-of-phase (χ_M'') ac susceptibility components measured at different frequencies for compound **1** at zero dc field and an oscillation of 2.5 Oe.

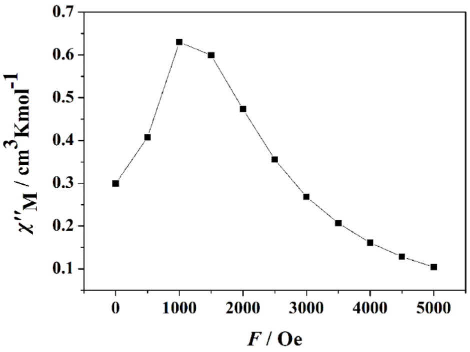

Fig. S7 Filed dependence of the out-of-phase (χ_M'') ac susceptibility components measured for compound **1** at 2 K from 0 Oe to 5000 Oe.

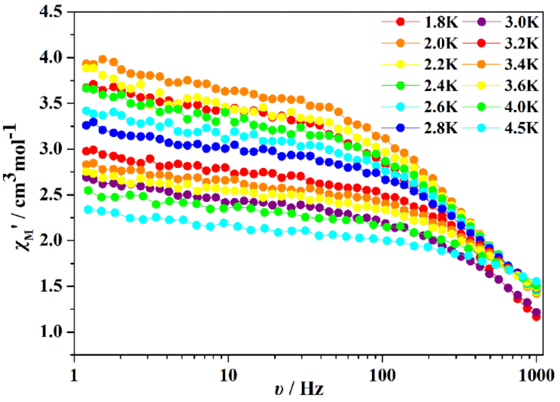

Fig. S8 Frequency dependence of the in-phase (χ_M') ac susceptibility components measured for compound **1** at 1000 Oe.

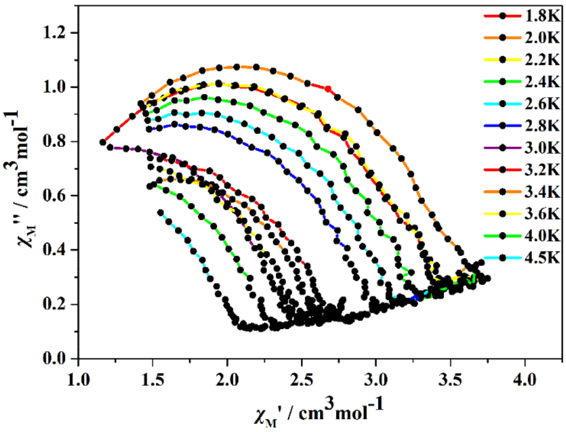

Fig. S9 Cole-Cole plots for **1**